



# Irreversible Thermodynamic Bound for the Efficiency of Light-Emitting Diodes

Jin Xue, Zheng Li, and Rajeev J. Ram

*Department of Electrical Engineering and Computer Science, Massachusetts Institute of Technology,  
Cambridge, Massachusetts 02139, USA*

(Received 26 July 2016; revised manuscript received 18 April 2017; published 20 July 2017)

A thermodynamic model for light-emitting diodes (LEDs) is developed by considering energy and entropy flows in the system. Thermodynamic constraints have previously been considered separately for the reversible process of electroluminescence in LEDs and for light extraction and collimation in other optical systems. By considering both processes in the LED model, an irreversible upper bound for the conversion of electrical energy to optical energy is derived and shown to be higher than unity, but tighter and more realistic than the reversible case. We also model a LED as an endoreversible heat engine where the carrier-transport processes can be directly connected to the elements of a thermodynamic cycle.

DOI: [10.1103/PhysRevApplied.8.014017](https://doi.org/10.1103/PhysRevApplied.8.014017)

## I. INTRODUCTION

The wall-plug efficiency (WPE) of modern light-emitting diodes (LEDs), which is defined as the ratio of optical output power to the electrical input power, has far surpassed all other forms of lighting and is expected to improve further as the lifetime cost of energy consumption exceeds the manufacturing cost of the devices. For instance, a recent report demonstrates WPE exceeding 80% for a gallium-nitride-based LED [1], which inevitably leads to questions about further enhancement towards the conventional limit of unity efficiency. Nevertheless, theory and experiments suggested that for light-producing devices such as LEDs, the WPE may exceed unity in practice [2–13] since the incoherent electroluminescent radiation emitted has finite entropy. Therefore, according to the second law of thermodynamics, LEDs can absorb net heat from the lattice and convert this energy to photons as long as the total entropy in the system does not decrease during steady-state operation. In this manner, the electrical part of the input power may be lower than the output optical power, and such LEDs can indeed work as a light-producing refrigerator.

Similar to the *etendue* conservation of ideal optical systems and Shockley-Queisser limit of photovoltaic cells [14,15], the efficiency limit of LEDs has been mainly studied in terms of thermodynamic and statistical analysis [3–8]. Planck [16] first calculated the entropy content of an ideal Bose gas in thermal equilibrium and introduced the temperature definition of quantum resonators occupied by bosons more than a century ago. Later, Landsberg [17] extended the application of this entropy calculation of a Bose gas to the near-equilibrium case. Landau [18] studied the limitations of photoluminescence imposed by thermodynamics and found that the luminescent output power may exceed the photoexcitation input. A similar investigation of the case of electroluminescence was reported by Weinstein [3] in 1960 and the accompanying cooling effect by Dousmanis *et al.* [4] in 1964. Then in 1968, an extended

discussion was finally brought up by Landsberg and Evans [5] to address the efficiency limit specifically for LEDs.

Other researchers have investigated the thermodynamic bound of energy-conversion efficiency for photoluminescence and electroluminescence in the reversible limit [3–8,18]. Here, we propose a tighter bound of the efficiency by considering a thermodynamic irreversibility associated with optical extraction, which is already known as *etendue* and radiance constraints in the context of passive optical systems [14]. If we consider the steady-state photon-extraction process from within the LED to the far field of the LED being a passive optical system, we show that the temperature of the internal radiation field within the LED is higher than that in the far field. This higher temperature demands more work to be done by the power supply to sustain the electroluminescence and, hence, lowers the WPE compared to the ideal reversible case. In the present paper, an irreversible thermodynamic model for energy conversion in a LED is constructed by considering the entropy and temperature of the internal and far-field radiation fields.

## II. THEORY

In the following, basic rate equations for energy and entropy change are presented first for the LED internal radiation field and then separately for the electronic system in order to derive an upper bound of WPE in the reversible limit. After converting the upper bound to a form associated with the temperature of far-field radiation, we see that an ideal forward-biased LED can be interpreted as a reversed Carnot engine. Then, through an analysis revealing the imbalance of the temperatures for the radiation field inside and outside a LED, an irreversible thermodynamic model is further developed for a LED in steady-state operation, as well as a tighter bound of the WPE.

Consider a LED die with a planar top-emitting structure. We investigate an open system consisting of the electrons within the device. In forward-biased steady-state operation,

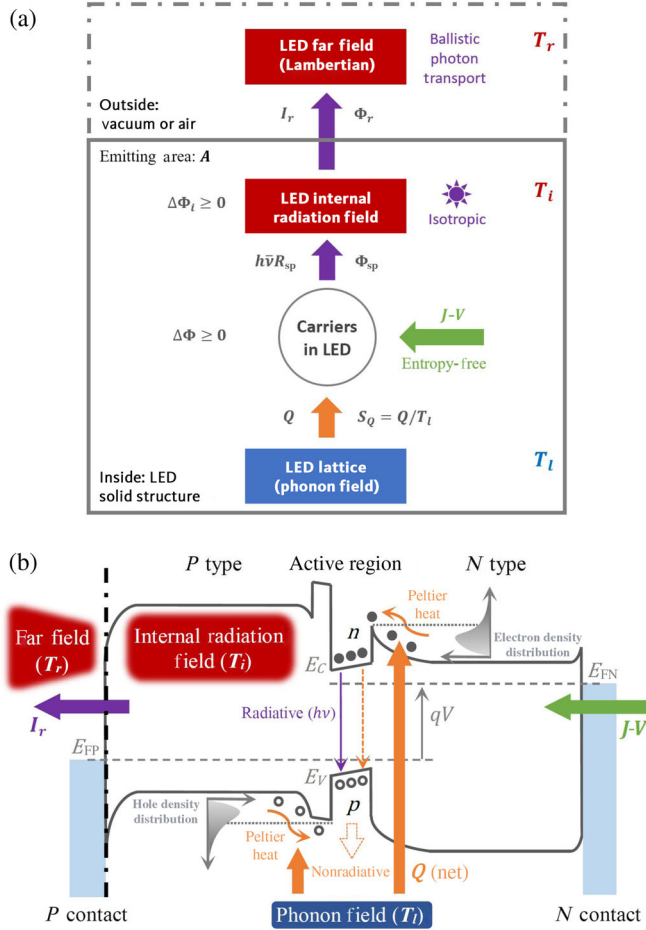


FIG. 1. (a) Block diagram showing the irreversible thermodynamic model of a LED. (b) Energy-band structure of a typical single-quantum-well LED under forward bias. The color scheme adopted for different types of energy input or output processes is consistent in (a) and (b).

the system is electrically pumped by entropy-free input work at the rate  $J-V$  per unit area (where  $J$  is the current density and  $V$  is the bias voltage) and emits electromagnetic energy through spontaneous radiative recombination at the net rate (per unit area)  $R_{sp}$  from the active region to the surrounding region, where the radiation is assumed to be distributed isotropically within the LED, as shown in Fig. 1(a). We further assume there is *no internal loss*; thus, the net radiation power leaving the LED from its internal radiation field through the top emitting surface (per unit area) denoted as  $I_r$  must equal  $h\bar{\nu}R_{sp}$  in the steady state, i.e.,

$$\frac{1}{A} \frac{dE_{r,i}}{dt} = h\bar{\nu}R_{sp} - I_r = 0, \quad (1)$$

where  $h$  is Planck's constant,  $\bar{\nu}$  is the mean photon frequency,  $A$  is the emitting area of the LED die, and  $E_{r,i}$  is the total energy of the internal radiation field. However, according to the second law of thermodynamics,

the net rate of entropy leaving the electronic system carried by  $h\bar{\nu}R_{sp}$  denoted as  $\Phi_{sp}$  must be less than or equal to that leaving the LED from the internal radiation field denoted as  $\Phi_r$ , i.e., in the steady state,

$$\frac{1}{A} \frac{dS_{r,i}}{dt} = \Phi_{sp} + \Delta\Phi_i - \Phi_r = 0, \quad (2)$$

where  $S_{r,i}$  is the total entropy of the internal radiation field, and  $\Delta\Phi_i$  is a non-negative entropy generation rate of the internal radiation field (per unit projected area) corresponding to any irreversible processes, which can arise from disordered scattering due to interactions with defect centers or a roughened backside mirror. In such a configuration, if ignoring all boundary effects between the LED emitting surface and the ambient, the far-field radiation pattern from the LED will be Lambertian, and the optical intensity scales with the inverse square law as the distance increases from the observer to the LED. In the analysis presented here, all the radiation power and associated entropy refer to the electroluminescence only. Effects from the background thermal radiation of the LED are negligible due to detailed balance with the ambient.

Along with the process of minority-carrier injection, the electronic system also absorbs heat from the lattice at the net rate  $Q$  per unit area due to the Peltier effect near the diode junction. This heat-transfer process is related to the restoration of the carrier distribution and is assumed to take place sufficiently close to the quasineutral regions of the LED, where carrier temperature can be considered the same as that of the lattice due to fast electron-phonon scattering processes. The energy-band diagram for a typical single-quantum-well LED depicting this process is shown in Fig. 1(b). The LED lattice serves as a phonon reservoir with temperature  $T_l$ . Thus, the net entropy transfer rate into the electronic system carried by  $Q$  is approximately  $Q/T_{e|inj} \approx Q/T_l$ , where  $T_{e|inj}$  is the electron temperature during the injection process. We can write two rate equations in the steady state for the  $E_{el}$  and  $S_{el}$  be the total internal energy and entropy of the electronic system described above,

$$\frac{1}{A} \frac{dE_{el}}{dt} = J-V + Q - h\bar{\nu}R_{sp} = 0, \quad (3)$$

$$\frac{1}{A} \frac{dS_{el}}{dt} = \frac{Q}{T_l} + \Delta\Phi - \Phi_{sp} = 0, \quad (4)$$

where  $\Delta\Phi$  is the internal entropy generation rate (per unit area) in the electronic system, which is also non-negative due to irreversible processes associated with nonideal LED operation such as nonradiative recombination, Joule heating, etc. Combining Eq. (1) with Eq. (4) with the second law of thermodynamics, we arrive at the following inequality:

$$\Delta\Phi + \Delta\Phi_i = \Phi_r - \frac{I_r - J - V}{T_l} \geq 0. \quad (5)$$

Thus, the WPE of a LED denoted as  $\eta_{\text{WP}}$  must satisfy

$$\eta_{\text{WP}} = \frac{I_r}{J - V} \leq \frac{I_r}{I_r - T_l \Phi_r}. \quad (6)$$

According to Eq. (6), the WPE of a LED has an upper bound that is dependent on the specific operating condition, and the bound is always greater than unity. This result is because the incoherent electroluminescence of LEDs contains finite entropy, but the input electrical work does not. The second law of thermodynamics then allows the LED electronic system to absorb some heat (with entropy accompanied) from the lattice. In the extreme case in which the entropy influx carried by the heat absorbed exactly balances the quota imposed by that of the output electroluminescence, the upper bound of WPE is achieved.

A calculation of  $\Phi_r$  is required to determine this bound for a given  $I_r$ . Assume  $f_i(\nu)$  to be the mean value of photon occupancy per mode at frequency  $\nu$  for the internal radiation field. The distribution of  $f_i$  over the frequency range of interest depends on the LED emission spectrum and the total radiation power leaving the LED,

$$I_r = \frac{c}{4n} \int h\nu f_i(\nu) g_i(\nu) d\nu, \quad (7)$$

where  $g_i(\nu)$  is the density of optical modes per unit volume for the internal radiation field,  $c$  is the vacuum light speed, and  $n$  is the refractive index of relevant material. Since the internal radiation field is assumed isotropic, the coefficient  $1/4$  is introduced from an integration related to the apparent area of emitting surface viewed by optical modes in different directions, similar to the case of poking a hole on the cavity of an ideal radiator. This coefficient is subject to change if there is an index difference across the emitting interface, in which case, the light escape cone shrinks. Then, given the entropy formula of an ideal Bose gas [16,17], the net rate of entropy leaving the LED carried by  $I_r$  can be written as

$$\Phi_r = \frac{c}{4n} \int k_B \{ [f_i(\nu) + 1] \ln [f_i(\nu) + 1] - f_i(\nu) \ln [f_i(\nu)] \} g_i(\nu) d\nu, \quad (8)$$

where  $k_B$  is the Boltzmann constant. Combining Eqs. (7) and (8),  $\Phi_r$  can be obtained for any given  $I_r$  and its spectral information. It is notable that the above construction of  $\Phi_r$  assumes that all photons in a small frequency interval are uniformly distributed among all the optical modes available; i.e., all photons (of the same frequency) have the same probability to occupy any of the modes despite the number of photons already in that mode. This assumption is *similar* to the thermal equilibrium condition of the internal radiation

field within each small frequency interval; thus  $\Phi_r$  is maximized for a given  $I_r$  together with its relative intensity spectrum. This assumption may be further extended such that the total incoherent electroluminescence produced by a LED has an intensity distribution of  $I_r(\nu)$  over a certain spectral interval close to that of a blackbody radiation. Given the above assumptions, a temperature definition for the electroluminescent radiation field naturally arises.

Assigning a temperature to the external radiation field (i.e., far field) of the LED has engendered much discussion in the literature [3,5,7]. Unlike the internal field, the external field itself is comprised of a ballistic ensemble of photons moving away from the device and is not in quasiequilibrium with the electrons and holes in the LED active region. Several authors have introduced a temperature definition for this external radiation field by considering the ratio between the energy and entropy flux leaving the LED, which is physically more like a characterization of heat transfer (i.e., the radiation close to the LED emitting surface) rather than a direct description of a thermal equilibrium system:

$$T_f(\nu) = \frac{I_r(\nu)}{\Phi_r(\nu)}. \quad (9)$$

For convenience, we can define a collective temperature to cover the entire spectrum of the far field in a similar way, denoted as  $T_r$ ,

$$T_r = \frac{I_r}{\Phi_r}. \quad (10)$$

This collective far-field temperature does not necessarily equal the result in Eq. (9) for each small frequency interval. In fact, the ratio in such a form is commonly used in entropy balance equations for open systems to describe the temperature at the point of a heat flow [19]. In the literature studying thermodynamics of light, it was also referred to as “effective temperature” [3] or “flux temperature” [7]. Weinstein [3] argued that  $I_r(\nu)/\Phi_r(\nu)$  is very nearly equal to the temperature of a blackbody which would have the same emission power in the band and physically interpreted it as a “brightness temperature”.

Applying the definition (10) to Eq. (6), we have

$$\eta_{\text{WP}} \leq \frac{T_r}{T_r - T_l}, \quad (11)$$

which is consistent with the result previously published by Weinstein [3]. In addition, we find the inequality in Eq. (11) matches the expression of the coefficient of performance for a classical heat pump operating between a cold and a hot reservoir with temperature  $T_l$  and  $T_r$ , respectively. Therefore, in the thermodynamic perspective, a forward-biased LED operating in the reversible limit can be considered equivalently as a reversed Carnot engine with its electronic system being the working fluid, lattice

structure (i.e., the phonon field) being the low-temperature reservoir, and far-field radiation (i.e., the photon field described above) being the high-temperature reservoir. The four-step reversed Carnot cycle leads to a net effect by which charged carriers consume external electrical work to pump heat from the LED lattice and release electroluminescence to the ambient.

So far, we have constructed and inspected the reversible thermodynamic model for a LED in the steady state. However, we have to be cautious and check whether the reversible limit is theoretically achievable, which requires (quasi) thermal equilibrium between the internal

and external radiation fields, since the LED electronic system directly interacts only with the internal field rather than the far field [i.e., the internal field should serve as an intermediate photon reservoir bridging the LED electronic system and the far field for them to interact reversibly at the temperature  $T_f(\nu)$ ]. And even if it is valid, we still need to check whether a practical LED far field truly has a temperature given in Eq. (10), as it was previously proposed in the literature.

The following is an examination of the spectral temperature of the internal radiation field, which is denoted as  $T_i(\nu)$  and defined by

$$T_i(\nu) = \frac{d[u(\nu)]}{d[s(\nu)]} = \frac{d[h\nu f_i(\nu)g_i(\nu)\Delta\nu]}{d(k_B\{[f_i(\nu) + 1]\ln[f_i(\nu) + 1] - f_i(\nu)\ln[f_i(\nu)]\}g_i(\nu)\Delta\nu)} = \frac{dI_r(\nu)}{d\Phi_r(\nu)}, \quad (12)$$

where  $u(\nu)$  and  $s(\nu)$  are the spectral energy and entropy density of the internal radiation field, respectively. Alternatively,  $T_i(\nu)$  can be directly calculated from  $f_i(\nu)$  by the Bose-Einstein distribution (with zero chemical potential) as well, which is equivalent to Eq. (12). The convexity of the entropy function of radiation indicates that  $T_i(\nu)$  from Eq. (12) is always larger than  $T_f(\nu)$  from Eq. (9) for the same frequency, and the ratio between them increases with increasing  $I_r(\nu)$ . A simple way to think about this mechanism is that for the internal radiation field, only photons contained in modes directed towards the emitting surface can escape from the LED cavity and become distributed in the far field. Therefore, together with the increased density of optical modes and conserved photon flux after the emission, the mean photon occupancy in the far field of the LED is always smaller than that inside. If also considering the ballistic transport nature of the external radiation flux (i.e., similar to the case of heat transfer), the far field can, thus, be assigned a lower temperature as defined in Eq. (10). On the other hand, the photon redistribution induced by the increasing of density of the quantum modes in an unconfined space (i.e., the ambient) justifies the entropy generation (or entropy maximization) during the optical extraction process, which may be caused by randomized scattering due to interactions with an imperfect dielectric interface. Hence, the etendue of the radiation can increase after being extracted from the LED, and, thus, the output radiance reduces, which matches the argument of temperature reduction in the far field. More important, in this situation the exact physical correspondence of  $I_r(\nu)/\Phi_r(\nu)$  to a (effective) temperature or how a practical LED far field reaches this temperature no longer matters, since the

intermediate photon reservoir—the internal radiation field—has a higher occupancy (temperature) and is better approximated as a system in quasiequilibrium with the distribution of electrons and holes in the LED's active region (more details can be found in Appendix A).

Since  $T_f(\nu) \neq T_i(\nu)$  for any frequency, the reversible limit and the efficiency bound in Eq. (11) cannot be achieved. As a result, similar to the treatment of an endoreversible heat engine (Novikov engine or Curzon-Ahlborn engine, to be more specific) [20–22], the electronic system of the LED must operate against  $T_i(\nu)$  rather than  $T_f(\nu)$  during the radiative recombination process, which is interpreted as the introduction of an irreversibility into the ideal reversible model. In other words, this semi-ideal thermodynamic configuration still consists of a fully reversible Carnot-like cycle in which the LED electronic system pumps heat from the lattice temperature (low) to the temperature of the internal field (high). With the LED emitting surface being an effective heat exchanger, the internal field is then coupled irreversibly with the far field of lower temperature to achieve a finite radiation power. This interpretation is reasonable, as any useful LED must have a finite output, and its electronic system should directly interact with the internal radiation field, not any far field. In addition, higher LED output intensity  $I_r$  always corresponds to (or is driven by) a larger temperature difference between the internal and the external radiation fields, which can be viewed as a stronger irreversibility. This observation is consistent with the basic characteristics of endoreversible engines. Therefore, a collective temperature definition covering the entire spectrum for the internal radiation field is defined as

$$T_i = \frac{d[\int u(\nu)d\nu]}{d[\int s(\nu)d\nu]} = \frac{d[\int h\nu f_i(\nu)g_i(\nu)d\nu]}{d(\int k_B\{[f_i(\nu) + 1]\ln[f_i(\nu) + 1] - f_i(\nu)\ln[f_i(\nu)]\}g_i(\nu)d\nu)} = \frac{dI_r}{d\Phi_r}. \quad (13)$$



Substituting for the temperature of hot reservoir in Eq. (11), now we have

$$\eta'_{\text{WP}} = \frac{I_r}{J-V} \leq \frac{T_i}{T_i - T_c}. \quad (14)$$

Since  $T_i > T_r$ , Eq. (14) provides a tighter and also more realistic bound than that in Eq. (11). It is notable that different from a typical Curzon-Ahlborn efficiency, which is obtained from a similar thermodynamic configuration (heat engine rather than the heat-pump model in this case) but specifically corresponds to a system condition of maximum output power, here  $\eta'_{\text{WP}}$  does not carry this meaning, as  $T_i$  is determined by the actual rate of heat transfer (i.e.,  $I_r$  and  $\Phi_r$ ) rather than being optimally chosen. In this case, different LED outputs yield different  $\eta'_{\text{WP}}$  according to Eq. (14). In addition, we can plot a temperature-entropy ( $T$ - $S$ ) diagram for the above irreversible LED model to identify each thermodynamic process it implements, which we further discuss in Appendix B.

Although we use the collective temperature as defined in Eq. (10), we can obtain a similar limit by considering the temperature of the far field for each frequency component,  $T_f(\nu)$ . The reversible limit of WPE can be derived for each small frequency interval within the spectral range of interest through the monochromatic version of Eq. (11). If we replace  $T_f(\nu)$  with  $T_i(\nu)$  in the equation, the irreversible limits at those frequencies are obtained, whose weighted average by the LED spectral profile leads to an overall upper bound of the WPE similar to Eq. (14). Therefore, given the radiation flux density of a LED (i.e.,  $I_r$ ) being properly measured for a  $2\pi$  solid angle close to the emitting surface, the irreversible limit calculated by Eq. (14) should serve as a good approximation for the upper bound of WPE. Also, the initial isotropic assumption of the internal radiation field, which allows us to assume a maximum entropy for the electroluminescent radiation, justifies the definition of the temperature. However, the key part of the arguments should still remain valid without this assumption as long as the gradient of photon occupancy exists between the optical modes of the internal and far-field radiation fields. For the special cases of anisotropic internal radiation fields, such as LEDs with a strong Purcell effect or of small dimension compared to the photon wavelength, the total entropy of the output electroluminescence will be overestimated by this model, as will the upper bound of WPE. In principle, Eq. (6) is universally applicable as long as the rate of total radiation entropy can be properly estimated.

### III. RESULTS AND DISCUSSION

Finally, let us examine the thermodynamic bound of WPE for typical LEDs operating with useful output powers. Here, the steady-state electroluminescence produced by LEDs is assumed to have a Gaussian spectral

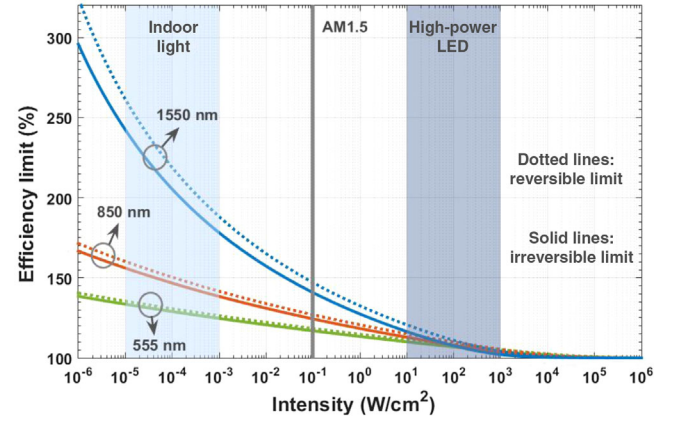


FIG. 2. The upper bound of WPE (at 300 K) for LEDs of 555-nm central wavelength with 20-nm full width at half maximum (FWHM), 850-nm central wavelength with 40-nm FWHM, and 1550-nm central wavelength with 100-nm FWHM are shown in green, red, and blue, respectively, with dotted lines representing the reversible limit from Eq. (11) and solid lines for irreversible limit from Eq. (14).

profile regardless of the exact LED operating condition, which is close to the actual case. For any given (or measured) optical intensity  $I_r$  with a Gaussian spectrum, we can first use Eq. (7) to retrieve the occupancy function  $f_i(\nu)$  for the internal radiation field and then put it into Eq. (8) to calculate the associated entropy flux  $\Phi_r$  of the total output. By applying Eqs. (10) and (11), a corresponding reversible bound of WPE is, thus, obtained, and the same for the irreversible bound by applying Eqs. (13) and (14). In Fig. 2, the upper bound of WPE for LEDs of different spectral profiles is plotted against a wide range of optical intensities, as it is a major dependence of the LED efficiency both empirically and theoretically. This plot indicates that LEDs can be much more efficient at lower optical intensity or longer emission wavelength, since the corresponding electroluminescence contains more entropy per unit optical power, allowing a higher ratio of heat influx to participate in carrier excitation. This trend has an exception at extremely high brightness. In addition, the maximum of WPE is unbounded when the intensity diminishes. For typical visible or infrared LEDs, the WPE in the reversible case can be as high as 130% to 250% at moderate brightness close to the indoor lighting condition, which is significantly higher than the conventional efficiency limit of unity. Even in the extremely high-power condition near  $100 \text{ W/cm}^2$ , the output intensity can still nontrivially surpass the electrical input power by more than 5%, with the remaining energy drawn from the LED lattice. More important, the irreversible limit, as expected from our model, is always lower than the reversible one of the same condition. This correction to the theoretical upper bound of WPE becomes increasingly more conspicuous and necessary at longer wavelength.

At last, we clarify that by indicating the internal radiation field, we are referring to the electromagnetic field distributed within the entire solid structure of the LED die. If any packaging material (e.g., solid immersion lens) is attached to the LED die, it can also be counted towards the internal volume, but in this case, the photon field within the packaging material is characterized by the same internal temperature  $T_i$  according to the model. Otherwise, if the LED package has very different structure or material properties, another intermediate radiation field may be further introduced accordingly, so as another irreversible process of photon coupling. By indicating the far field, we are referring to the ambient, which is typically vacuum or air.

### ACKNOWLEDGMENTS

This work is supported by Professor Amar G. Bose Research Grants and Fellowship from Agency for Science, Technology and Research, Singapore.

### APPENDIX A: ALTERNATIVE MANIFESTATION FOR THE QUASIEQUILIBRIUM CONDITION IN A LED

Suppose that the electron and hole density in the LED active region under bias voltage  $V$  and current density  $J$  is  $n$  and  $p$ , respectively, as shown in Fig. 1(b). Instead of treating the LED being electrically pumped to achieve high carrier density, if these hot carriers are imagined to be solely thermally excited by a high junction temperature  $T_j$ , we have

$$\begin{aligned} np &= N_C N_V \exp\left(-\frac{E_C - (E_i + \frac{1}{2}qV)}{k_B T_l}\right) \\ &\times \left(-\frac{(E_i - \frac{1}{2}qV) - E_V}{k_B T_l}\right) \\ &= N_C N_V \exp\left(-\frac{E_C - E_i}{k_B T_j}\right) \exp\left(-\frac{E_i - E_V}{k_B T_j}\right), \quad (\text{A1}) \end{aligned}$$

where  $N_C$  and  $N_V$  are the effective density of states at the conduction- and valence-band edge, respectively.  $E_C$  and  $E_V$  are the energy levels of the conduction- and valence-band edge, respectively.  $E_i$  is the intrinsic Fermi level, and  $q$  is the electron charge. Equation (A1) assumes an undoped active region of the LED, which is a common case. Solving Eq. (A1) with relation  $E_C - E_i = E_i - E_V = \frac{1}{2}h\bar{\nu}$ , where  $\bar{\nu}$  is the mean frequency of emitted photons, we have an expression of the LED bias voltage,

$$V = \frac{h\bar{\nu}}{q} \left(1 - \frac{T_l}{T_j}\right). \quad (\text{A2})$$

Combining Eq. (A2) with current density  $J = qI_r/(h\bar{\nu})$ , the wall-plug efficiency of the LED can be calculated by its

definition in this alternative manner and is found to reduce to the exact same form as in Eq. (14) if  $T_j = T_i$ . This condition is not unreasonable since the hot carriers in the LED active region interact directly with the internal radiation field rather than the far field. This result manifests that the quasiequilibrium status can be maintained between the internal radiation field and the injected carriers of a certain density [determined by the LED bias as in Eq. (A2)] and also justifies the isothermal process (step 3) described in Appendix B.

### APPENDIX B: THERMODYNAMIC CYCLE AND T-S DIAGRAM OF TYPICAL LED OPERATION

A toy model for the thermodynamic cycle associated with a LED is presented below. We can plot a  $T$ - $S$  diagram for the irreversible LED model to identify and associate each thermodynamic process roughly with an appropriate carrier-transport counterpart, which is shown in Fig. 3.

In this scenario, step 1 can be considered an isothermal heat-absorption process based on the Peltier effect, which corresponds to the local thermalization (energy-redistribution) process of the electrons at quasineutral regions sufficiently close to the LED junction. This event is considered isothermal at lattice temperature  $T_l$  due to the fast electron-phonon scattering process relative to the speed of transport. Step 2 is a separate isentropic process without heat exchange, specifically describing electrons being excited and injected into the LED active region via electrical pumping. In this process, the external bias effectively reduces the potential barrier near the LED junction, resulting in a change of local electron distribution. This change of electron distribution can alternatively be reflected by assuming a higher junction temperature in a quasiequilibrium state, as described in Appendix A. Therefore, carrier temperature in the active region rises from  $T_l$  to  $T_i$  in this step (note, to characterize the excited

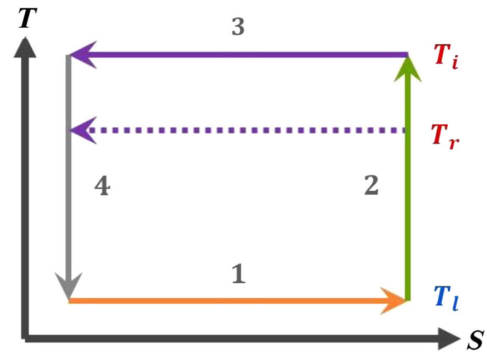


FIG. 3.  $T$ - $S$  diagram illustrating the thermodynamic cycle implemented by the irreversible LED model. In step 3, an extra dotted line is plotted in parallel to indicate the irreversibility introduced by the temperature difference between the LED internal radiation field ( $T_i$ ) and the far field ( $T_r$ ). The color scheme adopted here for different thermodynamic processes is consistent with those in Figs. 1(a) and 1(b).

state of carriers at  $T_i$ , the term “carrier temperature” was sometimes specified as “apparent radiant temperature” in the literature [8]). As electron-electron scattering tends to be faster than electron-phonon scattering, it may be reasonable to assume such a redistribution of electrons occurs after the injection. Step 3 is the other (approximately) isothermal process solely describing the radiative recombination event of injected electrons taking place in the LED active region that releases all the energy and entropy input from steps 1 and 2. This process is considered as isothermal at the hypothetically elevated junction temperature  $T_i$  since the electrons in the LED active region are in quasiequilibrium with the internal radiation field. As the last step, step 4 is the other isentropic process characterizing the temperature drop of some specific electrons from  $T_i$  back to  $T_l$  following the photon emission event. Therefore, it also implies a change of local electron distribution, which can be considered as a diffusive carrier-transport process leaving the LED junction for the other side of the quasineutral region after the interband transition (so they do not count towards leakage current). In this toy model, this step requires no net heat (entropy) exchange, thus, being approximated as an isentropic process. It also fulfills the current continuity requirement for the device. As a whole, the four parallel implementing processes as depicted (with solid lines) in the  $T$ - $S$  diagram form a reversible thermodynamic cycle of the electronic system, with an additional heat-exchange process represented by a dotted line indicating the irreversibility introduced to the LED model due to the temperature difference between the internal and external radiation fields.

---

[1] C. A. Humi, A. David, M. J. Cich, R. I. Aldaz, B. Ellis, K. Huang, A. Tyagi, R. A. DeLille, M. D. Craven, F. M. Steranka, and M. R. Krames, Bulk GaN flip-chip violet light-emitting diodes with optimized efficiency for high-power operation, *Appl. Phys. Lett.* **106**, 031101 (2015).  
 [2] J. Tauc, The share of thermal energy taken from the surroundings in the electro-luminescent energy radiated from a  $p$ - $n$  junction, *Czech. J. Phys.* **7**, 275 (1957).  
 [3] M. A. Weinstein, Thermodynamic limitation on the conversion of heat into light, *J. Opt. Soc. Am.* **50**, 597 (1960).  
 [4] G. C. Dousmanis, C. W. Mueller, H. Nelson, and K. G. Petzinger, Evidence of refrigerating action by means of

photon emission in semiconductor diodes, *Phys. Rev.* **133**, A316 (1964).  
 [5] P. T. Landsberg and D. A. Evans, Thermodynamic limits for some light-producing devices, *Phys. Rev.* **166**, 242 (1968).  
 [6] Y. P. Chukova, The region of thermodynamic admissibility of light efficiencies larger than unity, *Zh. Eksp. Teor. Fiz.* **68**, 1234 (1975).  
 [7] P. T. Landsberg and G. Tonge, Thermodynamic energy conversion efficiencies, *J. Appl. Phys.* **51**, R1 (1980).  
 [8] P. Berdahl, Radiant refrigeration by semiconductor diodes, *J. Appl. Phys.* **58**, 1369 (1985).  
 [9] O. Heikkilä, J. Oksanen, and J. Tulkki, Ultimate limit and temperature dependency of light-emitting diode efficiency, *J. Appl. Phys.* **105**, 093119 (2009).  
 [10] P. Santhanam, D. J. Gray Jr., and R. J. Ram, Thermoelectrically Pumped Light-Emitting Diodes Operating above Unity Efficiency, *Phys. Rev. Lett.* **108**, 097403 (2012).  
 [11] P. Santhanam, D. Huang, R. J. Ram, M. A. Remennyi, and B. A. Matveev, Room temperature thermos-electric pumping in mid-infrared light-emitting diodes, *Appl. Phys. Lett.* **103**, 183513 (2013).  
 [12] J. Xue, Y. Zhao, S. H. Oh, W. F. Herrington, J. S. Speck, S. P. DenBaars, S. Nakamura, and R. J. Ram, Thermally enhanced blue light-emitting diode, *Appl. Phys. Lett.* **107**, 121109 (2015).  
 [13] J. Oksanen and J. Tulkki, Thermophotonics: LEDs feed on waste heat, *Nat. Photonics* **9**, 782 (2015).  
 [14] J. Chaves, *Introduction to Nonimaging Optics*, 2nd ed. (CRC Press, Boca Raton, FL, 2015).  
 [15] W. Shockley and H. J. Queisser, Detailed balance limit of efficiency of  $p$ - $n$  junction solar cells, *J. Appl. Phys.* **32**, 510 (1961).  
 [16] M. Planck, in *Proceedings of Eight Lectures on Theoretical Physics* (Columbia University, New York, 1909).  
 [17] P. T. Landsberg, The entropy of a non-equilibrium ideal quantum gas, *Proc. Phys. Soc. London* **74**, 486 (1959).  
 [18] L. Landau, On the thermodynamics of photoluminescence, *J. Phys. USSR* **10**, 503 (1946).  
 [19] S. I. Sandler, *Chemical, Biochemical, and Engineering Thermodynamics*, 4th ed. (John Wiley & Sons, New York, 2006).  
 [20] I. I. Novikov, The efficiency of atomic power stations (a review), *J. Nucl. Energy II* **7**, 125 (1958).  
 [21] F. L. Curzon and B. Ahlborn, Efficiency of a Carnot engine at maximum power output, *Am. J. Phys.* **43**, 22 (1975).  
 [22] H. Ouerdane, Y. Apertet, C. Goupil, and P. Lecoeur, Continuity and boundary conditions in thermodynamics: From Carnot’s efficiency to efficiencies at maximum power, *Eur. Phys. J. Spec. Top.* **224**, 839 (2015).